Electronic Supplementary Material (ESI) for Lab on a Chip
This journal is © The Royal Society of Chemistry 2012

SUPPLEMENTAL INFORMATION
Increasing the detection speed of an all-electronic real-time biosensor

Matthew R. Leyden,[1] Robert J. Messinger,[2] Canan Schuman,[1] Tal Sharf,[1] Vincent T. Remcho,[3] Todd M. Squires,[2] and Ethan D. Minot[1]

[1] *Department of Physics, Oregon State University, Corvalis, OR, 97331, USA*
[2] *Department of Chemical Engineering, University of California, Santa Barbara, CA, 93106, USA*
[3] *Department of Chemistry, Oregon State University, Corvalis, OR, 97331, USA*
(Dated: December 20, 2011)

I. FINITE ELEMENT COMPUTATIONS

Governing equations. We model the convection, diffusion, and surface reactions of polylysine as occuring in a 2D channel, which is an excellent approximation since the width of the channel is much less than the width of the sensor ($W_\mathrm{c} \ll W_\mathrm{s}$). Polylysine both diffuses and advects with the fluid flow, obeying

$$\frac{\partial c'}{\partial t'} = D\nabla'^2 c' - \mathbf{u}' \cdot \nabla' c', \tag{1}$$

where c' is the local concentration, t' is time, D is the diffusivity, and $\mathbf{u}'$ is the local fluid velocity. A prime ($'$) indicates that a variable is dimensional. Unidirectional pressure-driven flow exhibits a parabolic velocity profile

$$\mathbf{u}'(y') = \frac{6Q}{W_\mathrm{c} H^3} y'(H - y')\hat{\mathbf{x}}, \tag{2}$$

where Q is the flow rate, W_c is the channel width, H is the channel height, y' is a spatial coordinate orthogonal to the sensor, and $\hat{\mathbf{x}}$ is a unit vector parallel to the sensor (Fig. S1).

For simplicity, and in the absence of evidence to the contrary, we assume that polylysine binds to the sensor via first-order Langmuir kinetics,

$$\frac{\partial b'}{\partial t'} = k_\mathrm{on} c'_\mathrm{s}(b_\mathrm{max} - b') - k_\mathrm{off} b', \tag{3}$$

where b' is the surface concentration of bound protein (units of molecules/area), k_on is the binding constant (volume/(molecules∗time)), c'_s is the protein concentration in the fluid above the sensor, b_max is the density of binding sites on the sensor (molecules/area), and k_off is the disassociation constant (1/time).

Boundary conditions. The boundary conditions for the different surfaces (Fig. S1) are

$$c' = c_0 \quad \text{at} \quad \text{surface A (inlet)} \tag{4}$$

$$\hat{\mathbf{n}} \cdot D\nabla' c' = 0 \quad \text{at} \quad \text{surfaces B (channel walls and outlet)} \tag{5}$$

$$\frac{\partial b'}{\partial t'} = -D\frac{\partial c'}{\partial y'} \quad \text{at} \quad \text{surface C (binding surface)}, \tag{6}$$

where $\hat{\mathbf{n}}$ is the outward unit normal vector from a surface. For clarity, Fig. S1 shows only a subset of the computational domain, since $H \gg \delta$, the depletion zone length. Boundary condition 4 requires that the incoming fluid has

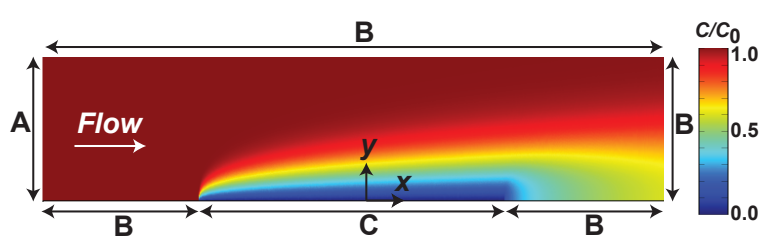

FIG. S1: Model of the CNT biosensor. The binding surface (including the sensor region) is represented by surface C.

concentration c_0 and boundary conditions 5 impose a 'no diffusive flux' at the channel walls and outlet. Boundary condition 6 relates the change in bound protein to the diffusive flux of polylysine to the sensor, linking eqns. 1 and 3.

The net flux J'_{D} is determined by integrating the rate of change of bound protein over the length of the sensor, or

$$J'_{\mathrm{D}} = W_{\mathrm{s}} \int_{-L/2}^{L/2} \frac{\partial b'}{\partial t'} dx'. \tag{7}$$

II. FUNDAMENTAL BOUNDARIES: THE REACTION- AND MASS TRANSPORT-LIMITS

Two extreme limits place boundaries on the binding curves [1]. One is the *reaction-limited* transport regime, where the reaction occurs so slowly that diffusion and convection are instantaneous by comparison. The concentration in the channel thus becomes c_0 everywhere, and eqn. 3 becomes

$$\frac{\partial b'}{\partial t'} = k_{\mathrm{on}} c_0 (b_{\mathrm{max}} - b') - k_{\mathrm{off}} b', \tag{8}$$

since $c'_{\mathrm{s}} \approx c_0$ and $\delta \approx 0$. Eqn. 8 can be solved to yield the Langmuir binding curve

$$\frac{b'(t')}{b_{\mathrm{max}}} = \frac{c_0/K_{\mathrm{D}}}{1 + c_0/K_{\mathrm{D}}} \left(1 - e^{-(k_{\mathrm{on}} c_0 + k_{\mathrm{off}})t'}\right), \tag{9}$$

where $K_{\mathrm{D}} = k_{\mathrm{off}}/k_{\mathrm{on}}$ is the equilibrium dissociation constant. Note that the number of molecules bound in equilibrium is $b_{\mathrm{equil}} = b_{\mathrm{max}}\tilde{c}/(1+\tilde{c})$, where $\tilde{c} = c_0/K_{\mathrm{D}}$. An example of a reaction-limited binding curve is given in Fig. S2a, which was obtained by solving eqn. 9 with $c_0 = 4$ nm (as used in Fig. 5c, main article), $k_{\mathrm{on}} = 10^9$ $\mathrm{M^{-1}s^{-1}}$, $k_{\mathrm{off}} = 10^{-3}$ $\mathrm{s^{-1}}$, and $b_{\mathrm{max}} = 2 * 10^{14}$ $\mathrm{m^{-2}}$. The choice of kinetic parameters is described below.

The *mass transport-limit* is where diffusion is rate limiting compared to the reaction. In this case $c'_{\mathrm{s}} \approx 0$, and the flux J'_{D} is constant in time, yielding $b' \approx J'_{\mathrm{D}} t' \approx (D c_0 W_{\mathrm{s}}/\delta) t'$. Examples of mass transport-limited binding curves are given in Fig. S2b, where all geometric and flow parameters are identical to those used in Fig. 5c of the main article. Kinetic parameters have been chosen such that the CNT sensor is completely mass transport-limited under these conditions, and are identical to those used in Fig. S2a. Here, both the CNT sensor before (black dashed curve with circles) and after (red dashed curve with circles) PEG deposition exhibit fluxes that are *constant* in time. Notably,

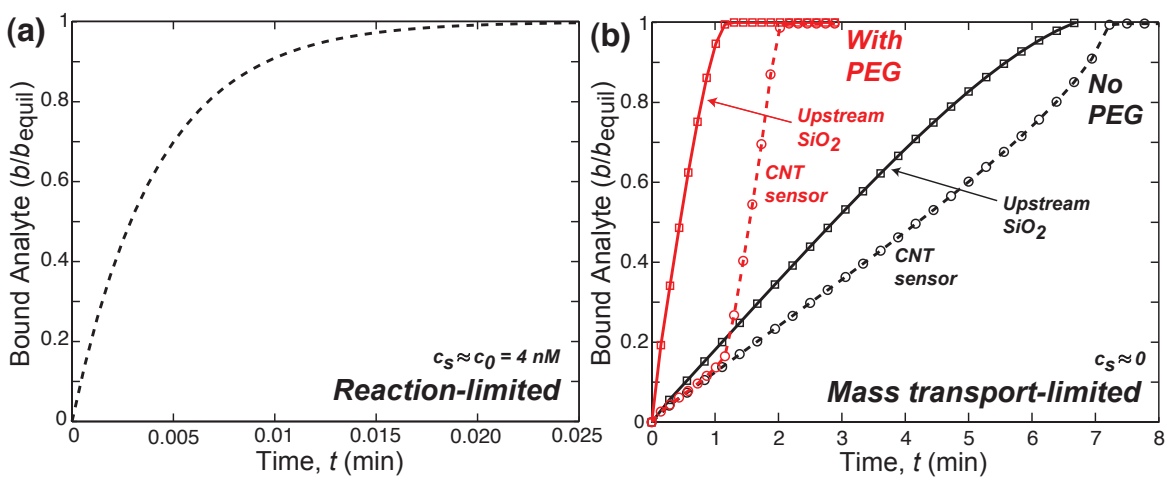

FIG. S2: The two fundamental sensing limits. (a) A reaction-limited binding curve with first-order Langmuir binding kinetics, obtained by solving eqn. 9 with $c_0 = 4$ nm, $k_{\mathrm{on}} = 10^9$ $\mathrm{M^{-1}s^{-1}}$, $k_{\mathrm{off}} = 10^{-3}$ $\mathrm{s^{-1}}$, and $b_{\mathrm{max}} = 2 * 10^{14}$ $\mathrm{m^{-2}}$. (b) A mass transport-limited binding curve, obtained by using identical kinetic parameters to the reaction-limited case, as well as identical flow and geometric parameters as those used in Fig. 5c in the main article. The CNT sensor before (black dashed curve with circles) and after (red dashed curve with circles) PEG deposition are shown, as well the upstream binding region before (black curve with squares) and after (red curve with squares) PEG deposition. Note that saturation of the upstream SiO_2 binding region changes the depletion zone length δ, thus increasing the diffusive flux to the sensor.

the adsorption of polylysine to the upstream SiO_2 binding region both before (black curve with squares) and after (red curve with squares) PEG deposition affects the flux to the sensor. For example, the binding curve for the CNT sensor after PEG deposition is 'kinked' at $t \approx 1.2$ min. This kink occurs when the binding region upstream of the sensor saturates, after which the binding region changes from $L \approx 1$ cm to ≈ 40 μm, and the depletion zone length δ becomes thinner and the diffusive flux increases. Overall, note the difference in characteristic shape between the binding curves for a mass transport-limited sensor (linear) compared to a reaction-limited sensor (exponential).

The time required to saturate the sensors in Fig. S2 reflects the choice of kinetic parameters, which have been selected here only to illustrate the fundamental limits imposed on the binding curves. Indeed, with these kinetic parameters, a CNT sensor with identical flow and geometric parameters to those in the main article would be mass transport-limited, saturating on the order of 1 to 10 min. In contrast, if it were possible to deliver polylysine to the sensor as fast as it could react, the CNT sensor would saturate on the order of 0.01 min.

Computationally, for a mass transport-limited sensor operating at steady-state (instantaneous adsorption and no sensor saturation), only eqn. 1 is solved subject to the boundary conditions 4, 5, and $c' = 0$ on surface C. Then, J'_{D} is determined by integrating the diffusive flux over the sensor surface,

$$J'_{\mathrm{D}} = -DW_{\mathrm{s}} \int_{-L/2}^{L/2} \frac{\partial c'}{\partial y'} dx'. \tag{10}$$

III. NON-DIMENSIONAL EQUATIONS

By non-dimensionalizing the above equations with appropriate scales for each variable, dimensionless parameters will emerge that represent ratios of competing effects. Such ratios characterize the important physics of the system (e.g., reaction-limited or mass transport-limited) and can be derived without detailed calculations. In addition, non-dimensionalization enables more efficient modeling, because one computation of a non-dimensionalized system represents a large number of experimentally-realizable scenarios.

The equation for fluid velocity (eqn. 2) is substituted into the equation governing polylysine concentration (eqn. 1) and subsequently non-dimensionalized. The concentration is scaled by the initial concentration ($c = c'/c_0$), the x-direction by the sensor length ($x = x'/L$), the y-direction by the channel height ($y = y'/H$), and time by the time required for the analyte to diffuse across the channel height ($t = Dt'/H^2$), yielding

$$\frac{\partial c}{\partial t} = \frac{1}{\lambda^2}\frac{\partial^2 c}{\partial x^2} + \frac{\partial^2 c}{\partial y^2} - \frac{6\mathrm{Pe_H}}{\lambda} y(1-y)\frac{\partial c}{\partial x}. \tag{11}$$

where $\mathrm{Pe_H} = Q/W_{\mathrm{c}}D$ and $\lambda = L/H$. The channel Péclet number $\mathrm{Pe_H}$ is a ratio of convective to diffusive flux, and characterizes whether the depletion zone δ above the sensor is thin ($\mathrm{Pe_H} \gg 1$) or thick ($\mathrm{Pe_H} \ll 1$) compared to the channel height H. Similarly, λ is a ratio of the sensor length L to the channel height H, and can be treated computationally using an anisotropic diffusivity.

For the Langmuir binding modeling (eqn. 3), the surface concentration b is non-dimensionalized by the maximum density of surface binding sites ($b = b'/b_{\mathrm{max}}$), and time and concentration are scaled as above, yielding

$$\frac{\partial b}{\partial t} = \epsilon\ \mathrm{Da}[\ c_{\mathrm{s}}(1-b) - \frac{1}{\tilde{c}}b], \tag{12}$$

where $\epsilon = c_0 H/b_{\mathrm{max}}$, $\mathrm{Da} = k_{\mathrm{on}} b_{\mathrm{max}} H/D$, and $\tilde{c} = c_0 k_{\mathrm{on}}/k_{\mathrm{off}} = c_0/K_{\mathrm{D}}$. The Damkohler number Da represents the ratio of reactive to diffusive flux, and characterizes whether the system is reaction-limited ($\mathrm{Da} \ll 1$, e.g., Fig S2a) or mass transport-limited ($\mathrm{Da} \gg 1$, e.g., Fig. S2b). The significance of ϵ and $\tilde{c}$, as well as additional analyses of Da, is discussed within ref. [1] below.

The boundary conditions 4 - 6 are also non-dimensionalized using the above scalings, yielding

$$c = 1 \quad \text{at} \quad \text{surface A (inlet)} \tag{13}$$

$$\hat{\mathbf{n}} \cdot D\nabla c = 0 \quad \text{at} \quad \text{surfaces B (channel walls and outlet)} \tag{14}$$

$$\frac{\partial b}{\partial t} = -\epsilon\frac{\partial c}{\partial y} \quad \text{at} \quad \text{surface C (binding surface)}, \tag{15}$$

The net flux J'_{D} is scaled by Dc_0W_{s}, resulting in a dimensionless flux $\mathcal{F}$ of polylysine to the sensor,

$$\mathcal{F} = \frac{Lb_{\mathrm{max}}}{H^2 c_0}\int_{1/2}^{1/2} \frac{\partial b}{\partial t} dx, \tag{16}$$

or for a mass transport-limited sensor operating at steady-state,

$$\mathcal{F} = -\lambda \int_{-1/2}^{1/2} \frac{\partial c}{\partial y} dx. \tag{17}$$

IV. INSIGHTS FROM FINITE ELEMENT COMPUTATIONS

Overall, comparisons of the experimental adsorption data with the finite element computations indicate that the CNT sensors in this work are neither strongly mass transport-limited nor reaction-limited, suggesting Da $\sim \mathcal{O}(1)$. The transient binding of polylysine to the CNT biosensor was modeled using eqns. 11 and 12 and boundary conditions 13-15. As given in the main article, $H = 100$ μm, $W_c = 200$ μm, $Q = 33$ μL/min, $c_0 = 4$ nm, and $D = 4 * 10^{-13}$ m^2/s. The length L of the binding region differs between an untreated and PEG-treated sensor. A perfectly PEG-passivated system has a 'bare' $L = 40$ μm binding region that consists of a 20 μm CNT 'sensing' region between two 10 μm electrodes that adsorb polylysine, but do not detect it. An untreated sensor has an additional $L = 1$ cm binding region of SiO_2 upstream of the CNT sensor.

While the geometric and flow parameters are known, the kinetic parameters k_{on}, k_{off}, and b_{max} are unknown. For the upstream binding region, we assume that binding between the highly positively charged polylysine and negatively charged SiO_2 is irreversible. Here, $k_{\text{off}} = 10^{-6}$ s^{-1} results in negligible desorption events over the course of the computations. The net charge density of the bare SiO_2 surface is $\sigma \approx -2.5$ μC/m^2 under the experimental salt and pH conditions, resulting in a polylysine b_{max} on the order of 10^{-14} m^{-2} by charge compensation. For the CNT sensor, the kinetic parameters for the 20 μm CNT 'sensing' region should be essentially identical to that of bare SiO_2, because the surface coverage of CNT's over the SiO_2 surface is small. We assume that the kinetic parameters between the polylysine and the two 10 μm metal electrodes are identical to that of the bare SiO_2. Thus, we use identical kinetic parameters when modeling both the 1 cm (upstream SiO_2) and 40 μm binding regions (CNT sensor).

As noted in the main article, PEG treatment of the device results in slight variations from ideal coverage, which furthermore can be measured. Quantitative fluorescent measurements indicate that (i) b_{max} of the CNT sensor reduces by 30% after PEG deposition, and (ii) b_{max} of the upstream SiO_2 region is 1/6 of the b_{max} of the untreated CNT sensor (and notably, not zero). These measured reductions in b_{max} are incorporated into the above models. Thus, the only remaining unknown parameters are k_{on} and b_{max} between polylysine and SiO_2.

To collectively reproduce the experimental adsorption data both before and after PEG deposition, the optimum kinetic parameters were $k_{\text{on}} = 10^{6.2}$ M^{-1}s^{-1} and $b_{\text{max}} = 6 * 10^{14}$ m^{-2}. For example, Fig. S3 shows the concentration of bound protein b, scaled by its equilibrium value b_{equil}, as a function of time both before (black curve, experiment; magenta curve, theory) and after (red curve, experiment; blue curve, theory) PEG deposition. The Langmuir binding curve (black dashed curve) illustrates the fundamental reaction-limit using these kinetic parameters. Note that

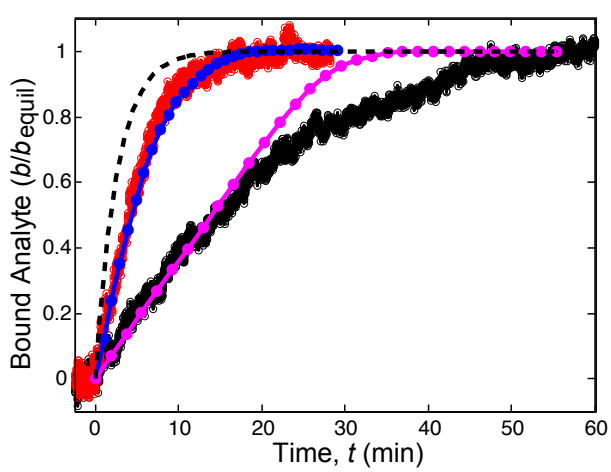

FIG. S3: Surface concentration of bound polylysine vs. time for the CNT biosensor both before (black curve, experiment; magenta curve, theory) and after (red curve, experiment; blue curve, theory) PEG deposition. Here, $k_{\text{on}} = 10^{6.2}$ M^{-1}s^{-1}, $k_{\text{off}} = 10^{-6}$ s^{-1}, $b_{\text{max}} = 6 * 10^{14}$ m^{-2}, and geometric and flow parameters are given above. The Langmuir binding curve (black dashed curve) represents the fundamental reaction-limit. Experimental data is scaled from Fig. 5c in the main article.

since the experimental binding curves are not reaction-limited (or there would be no flux enhancement upon PEG deposition), the Langmuir curve must saturate faster than the experimental data. The experimental binding curves are also not mass transport-limited, as evident by the measured non-linear flux of polylysine to the CNT sensor (compare to Fig. S2b), suggesting Da $\sim \mathcal{O}(1)$. Lastly, note that if the reaction between the polylysine and the SiO_2 was indeed mass transport-limited, a 'kink' in the binding curve would be observed for our system, similar to Fig. S2b. This observation is additional evidence that the CNT sensors operate in an intermediate regime that is neither strongly mass transport- or reaction-limited.

The modeling predicts the initial flux enhancement of 2.5 upon PEG deposition and reproduces the experimental results after PEG deposition, but not before it. The model before PEG deposition (magenta curve) overpredicts the experimental data (black curve) after approximately 15 min, thus resulting in early sensor saturation. Note that the experimental adsorption data can be modeled reasonably well, however, either before ($k_{\mathrm{on}} = 10^{5.4}$ $\mathrm{M^{-1}s^{-1}}$, $b_{\max} = 2 * 10^{14}$ $\mathrm{m^{-2}}$) or after PEG deposition ($k_{\mathrm{on}} = 10^{6.1}$ $\mathrm{M^{-1}s^{-1}}$, $b_{\max} = 2 * 10^{14}$ $\mathrm{m^{-2}}$). A few different reasons may explain why the above models do not collectively reproduce the adsorption data both before and after PEG deposition. For example, we assumed first-order binding kinetics between the polylysine and both the SiO_2 and CNT sensor as the simplest starting point. A more complicated adsorption process would require a different binding model. PEG contamination on the CNT sensor may also affect the kinetic rate constants. In addition, the kinetic parameters between the polylysine and the metal electrodes are unknown (also, fluorescence is quenched by the gold, so measurements of $b_{\max}$ by this method are not possible). Regardless, the computations suggest that additional ingredients may be needed to collectively model the experimental data both before and after PEG deposition.

While modeling the transient problem is insightful, the maximum flux enhancement limits upon PEG deposition can be determined by analyzing a completely mass transport-limited sensor. However, in order for such analyses to be valid, the system must evolve in a quasi-steady state.

V. QUASI-STEADY STATE

The system evolves in a quasi-steady state if the time to develop the depletion zone (t_δ) is fast compared to the time required to saturate the sensor (t_{sat}), or $t_\delta \ll t_{\mathrm{sat}}$. Note that t_δ is simply the time required for the polylysine to diffuse across the depletion zone, $t_\delta \sim \delta^2/D$. Here, $t_\delta \sim 4$ s for a 1 cm binding length (for which $\delta \sim 1.3$ μm) and $t_\delta \sim 0.1$ s for a 40 μm binding length (for which $\delta \sim 200$ nm). As seen from Fig. S3 and the Fig. 5c in the main article, t_{sat} is on the order of 10 min, which is much larger than t_δ for either the untreated or PEG-treated sensor. Thus, $t_\delta \ll t_{\mathrm{sat}}$, indicating that the CNT biosensors operate in the quasi-steady state regime.

VI. MAXIMUM FLUX ENHANCEMENT LIMITS

To compute the maximum flux enhancement of polylysine upon PEG deposition, we analyze a mass transport-limited sensor operating in the quasi-steady state regime. Physically, inhibiting polylysine adsorption on the upstream SiO_2 decreases the depletion zone thickness δ across which the protein must diffuse, increasing the flux to the sensor. Two dimensionless Péclet numbers, which represent competing ratios of convective to diffusive flux, characterize this depletion zone [1]. The channel Péclet number derived above compares δ to the channel height H. Here, $\mathrm{Pe_H} \sim 7*10^6 \gg 1$, indicating the depletion zone is extremely thin ($\delta \ll H$). The sensor Péclet, $\mathrm{Pe_S} = 6QL^2/H^2W_{\mathrm{c}}D$, characterizes δ relative to the length L of the binding surface. Since $\mathrm{Pe_S} \sim 4*10^{11}$ and $7*10^6$ for 1 cm (before PEG) and 40 μm (after PEG) binding regions, respectively, depletion zones are thinner than the binding lengths. Since $\mathrm{Pe_H}$ and $\mathrm{Pe_S} \gg 1$, the flux J_D to the sensor may be approximated following the work of Lévèque [2],

$$J_{\mathrm{D}} \approx 0.81 D c_0 W_{\mathrm{s}} \mathrm{Pe_S}^{1/3}[(\mathrm{b}/L)^{2/3} - (\mathrm{a}/L)^{2/3}], \tag{18}$$

where c_0 is the protein concentration, W_{s} is the sensor width, and $0 \leq a/L < b/L \leq 1$ is the sensor location within the binding region. As mentioned above, a perfectly PEG-passivated system has a $L = 40$ μm binding region that consists of a 20 μm CNT 'sensing' region between two 10 μm electrodes that adsorb polylysine, but do not detect it ($a/L = 1/4, b/L = 3/4$). By contrast, an untreated system has a binding length 10040 μm ($a/L = 101/104, b/L = 103/104$). Eqn. 18 yields $J_{\mathrm{D}} = 760$ and 6300 molecules/s to the CNT sensor before and after PEG deposition, respectively. Thus, the maximum flux enhancement one can achieve by passivating the upstream surface is 8.3 for a mass transport-limited device. Note that this result differs by less than 2% compared to the flux enhancement determined by our finite element computations of a mass transport-limited sensor operating at steady-state.

[1] T.M. Squires, R.J. Messinger and S.R. Manalis, *Nat. Biotech.*, 2008, **26**, 417–426.
[2] W.M. Deen, *Analysis of Transport Phenomena*, Oxford University Press: New York, 1998.